Am J Physiol Renal Physiol 293: F342–F349, 2007.
First published April 18, 2007; doi:10.1152/ajprenal.00004.2007.

Increasing or stabilizing renal epoxyeicosatrienoic acid production attenuates abnormal renal function and hypertension in obese rats

Hui Huang,[1,3] Christophe Morisseau,[2] JingFeng Wang,[3] Tianxin Yang,[4] John R. Falck,[5] Bruce D. Hammock,[2] and Mong-Heng Wang[1]

[1]*Department of Physiology, Medical College of Georgia, Augusta, Georgia;* [2]*Department of Entomology and Cancer Center, University of California, Davis, California;* [3]*Second Affiliated Hospital of Sun Yat-Sen University, Guangzhou, Guangdong Province, People's Republic of China;* [4]*Division of Nephrology, University of Utah and Veterans Affairs Medical Center, Salt Lake City, Utah; and* [5]*Departments of Biochemistry and Pharmacology, University of Texas Southwestern Medical Center, Dallas, Texas*

Submitted 3 January 2007; accepted in final form 10 April 2007

Huang H, Morisseau C, Wang JF, Yang T, Falck JR, Hammock BD, Wang M-H. Increasing or stabilizing renal epoxyeicosatrienoic acid production attenuates abnormal renal function and hypertension in obese rats. *Am J Physiol Renal Physiol* 293: F342–F349, 2007. First published April 18, 2007; doi:10.1152/ajprenal.00004.2007.—Since epoxyeicosatrienoic acids (EETs) affect sodium reabsorption in renal tubules and dilate the renal vasculature, we have examined their effects on renal hemodynamics and sodium balance in male rats fed a high-fat (HF) diet by fenofibrate, a peroxisome proliferator-activated receptor-α (PPAR-α) agonist and an inducer of cytochrome *P*-450 (CYP) epoxygenases; by *N*-methanesulfonyl-6-(2-proparyloxyphenyl)hexanamide (MSPPOH), a selective EET biosynthesis inhibitor; and by 12-(3-adamantane-1-yl-ureido)dodecanoic acid (AUDA), a selective inhibitor of soluble epoxide hydrolase. In rats treated with fenofibrate (30 $mg \cdot kg^{-1} \cdot day^{-1}$ ig) or AUDA (50 mg/l in drinking water) for 2 wk, mean arterial pressure, renal vascular resistance, and glomerular filtration rate were lower but renal blood flow was higher than in vehicle-treated control rats. In addition, fenofibrate and AUDA decreased cumulative sodium balance in the HF rats. Treatment with MSPPOH (20 $mg \cdot kg^{-1} \cdot day^{-1}$ iv) + fenofibrate for 2 wk reversed renal hemodynamics and sodium balance to the levels in control HF rats. Moreover, fenofibrate caused a threefold increase in renal cortical CYP epoxygenase activity, whereas the fenofibrate-induced elevation of this activity was attenuated by MSPPOH. Western blot analysis showed that fenofibrate induced the expression of CYP epoxygenases in renal cortex and microvessels and that the induction effect of fenofibrate was blocked by MSPPOH. These results demonstrate that the fenofibrate-induced increase of CYP epoxygenase expression and the AUDA-induced stabilization of EET production in the kidneys cause renal vascular dilation and reduce sodium retention, contributing to the improvement of abnormal renal hemodynamics and hypertension in HF rats.

obesity; cytochrome *P*-450; arachidonic acid; eicosanoid; kidney

CYTOCHROME *P*-450 (CYP) enzymes constitute a major metabolic pathway for arachidonic acid (AA). In the presence of NADPH and oxygen, AA is epoxidized by the CYP enzyme system to give four epoxyeicosatrienoic acids (EETs): 5,6-EET, 8,9-EET, 11,12-EET, and 14,15-EET. The EETs are hydrolyzed by soluble epoxide hydrolase (sEH) to the corresponding *vic*-dihydroxyeicosatrienoic acids (DHETs) (14, 21, 24).

EET biosynthesis can be carried out by several CYP isoforms, including the CYP1A, CYP2B, CYP2C, CYP2D, CYP2E, and CYP2J families (24). Although many CYP enzymes can epoxidize AA, it has been demonstrated that CYP2C and CYP2J are primarily responsible for renal EET formation. Holla et al. (11) showed that recombinant CYP2C11, CYP2C23, and CYP2C24, in that order, have the highest-to-lowest expoxygenase activity. Similarly, recombinant rat CYP2J3 and CYP2J4 are active in the metabolism of AA to EETs (25, 36, 38). Renal epoxygenase profiles and antibody inhibition studies have established that CYP2C23 is the predominant AA epoxygenase in the rat kidney (11). To study the physiological function of EETs, Falck et al. (32) synthesized selective CYP epoxygenase inhibitors such as *N*-methanesulfonyl-6-(2-proparyloxyphenyl)hexanamide (MSPPOH). The selective inhibition of EET production by MSPPOH has been demonstrated in vitro (32) and in vivo (17, 22, 40).

DHET is synthesized mainly from sEH, which is predominantly present in the cytosol and peroxisomes (30). DHETs are considered to be biologically less active than EETs. For example, the sEH product 11,12-DHET has no vasodilatory actions, whereas 11,12-EET dilates renal microvessels (13, 14). Therefore, many investigators used the inhibition of sEH activity to study the physiological functions of EETs. Using this strategy, Hammock and colleagues (27) synthesized several selective sEH inhibitors, including 12-(3-adamantane-1-yl-ureido)dodecanoic acid (AUDA), which have been used to examine the physiological function of EETs (5, 15, 27).

Obesity, which affects one in three Americans, is a serious health problem, because obesity often is associated with essential hypertension (8). Using different rat models, investigators demonstrated the link between obesity and hypertension (1, 3). For example, using the hypothalamic lesion-induced obese model, Baylis and colleagues (1) demonstrated that blood pressure is ~20 mmHg higher in obese male rats than in control rats. Similarly, using a high-fat (HF) feeding model, Dobrian and colleagues (3) showed that blood pressure is ~20 mmHg higher in obese male rats than in control rats. However, the mechanisms whereby obesity causes hypertension are not fully understood. To better understand those mechanisms, different investigators have used a rat model fed an HF diet (2,

Address for reprint requests and other correspondence: M.-H. Wang, Dept. of Physiology, Medical College of Georgia, Augusta, GA 30912 (e-mail: mwang@mail.mcg.edu).

The costs of publication of this article were defrayed in part by the payment of page charges. The article must therefore be hereby marked "*advertisement*" in accordance with 18 U.S.C. Section 1734 solely to indicate this fact.

4, 33). We have chosen this model because it mimics the effects of human HF-food consumption; rats develop characteristic features of human obesity-induced hypertension, including increased renal tubular reabsorption and glomerular filtration rate (GFR) (8). Moreover, the increased blood pressure in HF rats is associated with sodium retention (41), decreased expression of renal CYP epoxygenase, and decreased production of renal EETs (33, 42).

Since it has been demonstrated that EETs inhibit sodium transport in the nephron and cause vasorelaxation (24, 34, 39), we hypothesize that increased production of renal EETs can affect renal function and blood pressure in HF rats. To test this hypothesis, we used 11-wk-old HF rats to examine the effects of fenofibrate, a CYP epoxygenase inducer; MSPPOH, a selective EET biosynthesis inhibitor; and AUDA, a selective inhibitor of sEH. Specifically, we determined the effects of these agents on various renal functional parameters, including mean arterial pressure (MAP), renal blood flow (RBF), renal vascular resistance (RVR), GFR, and sodium balance.

MATERIALS AND METHODS

Materials. [1-^{14}C]AA (56 mCi/mmol) was obtained from Moravek Biochemicals (Brea, CA), the reagents for Western blot analysis from Amersham Bioscience (Piscataway, NJ), all HPLC solvents and chemicals for buffers from Sigma-Aldrich (Milwaukee, WI), and 20-hydroxyeicosatetraenoic acid (HETE), EETs, and DHETs from Cayman Chemicals (Ann Arbor, MI).

Animals. Male 3-wk-old Sprague-Dawley rats (Harlan, Indianapolis, IN) were divided into two groups. The experimental group of HF rats was fed a modified chow containing 36% fat (15.2% saturated and 20.8% unsaturated), 35% carbohydrate, 20% protein, and 0.4% salt (Bio-Serv, Frenchtown, NJ). Control rats were fed a normal rat chow containing 4.4% fat (2.5% saturated and 1.9% saturated), 46.6% carbohydrate, 24% protein, and 0.4% salt. All rats were maintained on a 12:12-h light-dark cycle and were housed two to a cage. All animal protocols were approved by the Institutional Animal Care and Use Committee and were in accordance with the requirements stated in the National Institutes of Health *Guide for the Care and Use Laboratory Animals*.

Determination of blood pressure in conscious HF and control male rats. After rats had been fed the HF or control diet for 8 wk, they were divided into a vehicle control group and four treatment groups, with six animals in each group. Rats in treatment groups were given fenofibrate (30 mg·kg^{-1}·day^{-1} in corn oil ig), fenofibrate (30 mg·kg^{-1}·day^{-1} in corn oil ig) + MSPPOH (20 mg·kg^{-1}·day^{-1} iv), AUDA (50 mg/l in drinking water), or MSPPOH (20 mg·kg^{-1}·day^{-1} iv). The fenofibrate dose of 30 mg·kg^{-1}·day^{-1} was based on a report by Muller et al. (20), who showed that, at this dose, fenofibrate selectively increases renal EET production in Sprague-Dawley rats. The MSPPOH dose of 20 mg·kg^{-1}·day^{-1} was based on our previous finding that, at this dose, MSPPOH selectively inhibits renal EET production in Sprague-Dawley rats (12). The AUDA dose of 50 mg/l in drinking water was based on personal communication with a colleague (Dr. J. D. Imig) who has extensive experience with AUDA at 25 and 50 mg/l in Sprague-Dawley rats and suggested that we use 50 mg/l for the maximal effect in HF rats. In a preliminary study, we found that AUDA at 25 mg/l did not significantly decrease blood pressure in HF rats. The procedure for dissolving AUDA in a hydroxypropyl-β-cyclodextran solution is described elsewhere (5, 37). After 2 wk of treatment, the blood pressure of these conscious, freely moving rats was determined through the femoral artery.

Determination of renal hemodynamics in treated HF rats. Eleven-week-old rats (n = 6) that had been fed the HF diet for 8 wk were treated with vehicle, fenofibrate, fenofibrate + MSPPOH, AUDA, or MSPPOH for 2 wk, and renal hemodynamics were measured. Each rat was weighed before surgery and anesthetized with 2% isoflurane via an anesthesia apparatus. One polyethylene cannula was placed in the trachea (PE-205) to allow free breathing, one in the bladder (PE-240) to collect urine, one in the femoral artery (PE-50) to measure and record MAP with a pressure transducer, and one in the femoral vein (PE-50) to infuse agents. Then infusion of saline (3 ml/h iv) and 0.5 ml of FITC-inulin (8 mg/ml in PBS; Sigma-Aldrich) over 2 min as a priming dose was initiated. A left laparotomy was performed, and a flow probe (Transonic System, Ithaca, NY) was placed over the left renal artery for measurement of RBF. The rat's body temperature was maintained at 37°C by a temperature controller (Cole Palmer Instrument) connected to a heating mat and a rectal temperature probe. After a volume of saline containing 6.2% of BSA equal to 1.25% of body weight had been infused, the intravenous infusion was switched to saline without BSA, but with FITC-inulin at 4 mg/ml. At least 45 min were allowed for equilibration after surgery before 30-min urine collections were begun. Arterial blood (0.4 ml) was drawn from the femoral artery in the middle of each 30-min clearance period for measurement of GFR. An equal volume of normal saline was infused for volume replacement. MAP, RBF, and RVR measurements were obtained from a computerized data collection-and-analysis system (EMKA Technologies, Falls Church, VA). A fluorescent plate reader (GENios Plus, Tecan, Research Triangle Park, NC) at 485-nm excitation and 538-nm emission was used to determine the concentration of FITC-inulin in plasma and urine for calculation of GFR, as described previously (23, 41).

Determination of sodium retention in treated HF rats. Eleven-week-old HF rats (n = 6) were treated with vehicle, fenofibrate, fenofibrate + MSPPOH, AUDA, or MSPPOH for 15 days. During treatment, these HF rats were kept in individual metabolic cages. Daily food intake, water intake, and urine volume were measured for determination of sodium balance. Sodium concentration was measured using an electrolyte system (Synchron EL-ISE, Beckman, Brea, CA). Daily sodium intake, excretion, and balance, as well as cumulative sodium balance, were calculated as described previously (9). After treatment, the rats were killed, and their kidneys were isolated for preparation of renal cortex and renal microvessels. These tissues were processed for immunohistochemical, Western blot, and AA metabolism analyses.

Immunohistochemical analysis. Kidneys from treated HF rats were isolated. A specimen cup containing 2-methylbutane was precooled for 45 min in a Styrofoam cooler containing dry ice and ethanol. The kidney slice was embedded in a specimen mold containing OCT compound (Miles Scientific, Naperville), which was placed in the cup for 2 min. The kidney samples were kept frozen at −80°C until they were sectioned. The samples were cut on a cryostat at a thickness of 10 μm and thawed onto glass slides. Specimens were fixed in cold acetone for 10 min at −20°C. To distinguish the expression of the different CYP isoforms, diaminobenzidine (DAB) was used to detect CYP2J, red fluorescence (tetramethylrhodamine isothiocyanate) to detect CYP2C23, and green fluorescence (FITC) to detect CYP2C11. For the DAB method, nonspecific binding sites were blocked by 2% normal rabbit serum in PBS, and endogenous peroxidase activity was blocked by 0.9% hydrogen peroxide in PBS for 1 h. The slides were rinsed with PBS and incubated with a 1:400 dilution of rabbit anti-human CYP2J2 antibody (a gift from Dr. D. C. Zeldin, National Institute of Environmental Health Science, Research Triangle Park, NC) for 12 h at room temperature. The slides were rinsed with PBS and covered with a 1:100 dilution of a biotinylated-coupled goat anti-rabbit secondary antibody for 30 min. An ABC kit (Vector Laboratories, Burlingame, CA) was used to stain the slides, which were developed for 3 min using a DAB kit (Vector Laboratories). For the fluorescence method, the slides were rinsed with PBS three times and then incubated with rabbit anti-CYP2C23 (1:600 dilution; Detroit R & D, Detroit, MI) or mouse anti-CYP2C11 (1:400 dilution; Detroit R & D) primary antibody. The slides were blocked with 3.3% normal

serum and then incubated with tetramethylrhodamine isothiocyanate-labeled goat anti-rabbit secondary antibody for CYP2C23 or FITC-labeled goat anti-mouse secondary antibody for CYP2C11. The slides were mounted with Vectashield (Vector Laboratories) and examined by fluorescence microscopy. Color and fluorescent images were quantified using Metamorph software (Universal Imaging, Downingtown, PA). For the negative control slides, the same procedure, without incubation with the primary antibody, was used.

AA metabolism. Renal cortical homogenates (150 μg) isolated from treated HF rats were incubated for 30 min at 37°C with [1-^{14}C]AA (0.4 μCi, 7 nmol) and NADPH (1 mmol/l) in 0.3 ml of PBS (100 mmol/l, pH 7.4) containing 10 mmol/l $MgCl_2$. After the reaction was terminated by acidification to pH 3.5–4.0 with 2 mol/l formic acid, AA metabolites were extracted with ethyl acetate. The ethyl acetate was evaporated under nitrogen, the metabolites were resuspended in 50 μl of methanol, and reverse-phase HPLC was performed as described previously (40). Identities of the AA metabolites (20-HETE, DHETs, and EETs) were confirmed with authentic standards. The activity of these metabolites was estimated on the basis of the specific activity of the added [1-^{14}C]AA and expressed as picomoles per milligram of protein per minute.

Western blot analysis. Renal microsomes (10 μg) from treated HF rats were separated by electrophoresis on an 8% SDS-polyacrylamide gel at 25 mA/gel at 4°C for 3 h. The proteins were electrophoretically transferred to an enhanced chemiluminescence membrane. The membranes were blocked with 5% nonfat dry milk in Tris-buffered saline (TBS) containing 10 mmol/l Tris·HCl, 0.1% Tween 20, and 150 mmol/l NaCl for 90 min and then washed three times with TBS. The membranes were incubated for 10 h with mouse anti-rat CYP2C11 (1:2,000 dilution; Detroit R & D), rabbit anti-rat CYP2C23 antibody (1:5,000 dilution; Detroit R & D), rabbit anti-human CYP2J2 antibody (1:2,000 dilution; a gift from Dr. D. C. Zeldin), or β-actin (1:5,000 dilution; Sigma Chemical, St. Louis, MO) at room temperature. The membranes were washed several times with TBS solution and further incubated with secondary antibody for these proteins. The immunoblots were developed using an enhanced chemiluminescence detection kit (Amersham, Arlington Heights, IL). The expression of these proteins was normalized to the expression of β-actin, as previously described (40).

Statistical analysis. Values are means ± SE. All data were analyzed by SPSS computer software (SPSS, Chicago, IL). The significance of differences in sodium balance between HF rats given different treatments was evaluated with ANOVA for repeated measurements followed by Tukey's multiple-range post hoc test. All other data were analyzed by one-way ANOVA or a Student's unpaired two-tailed test. Statistical significance was set at $P < 0.05$.

RESULTS

Effects of fenofibrate, MSPPOH, and AUDA on blood pressure in HF and control rats. To examine the effects of increased biosynthesis and stabilization of renal EET on blood pressure regulation, 11-wk-old HF and age-matched control rats fed a control diet were treated with vehicle, fenofibrate (30 mg·kg^{-1}·day^{-1} ig), fenofibrate (30 mg·kg^{-1}·day^{-1} ig) + MSPPOH (20 mg·kg^{-1}·day^{-1} iv), AUDA (50 mg/l in drinking water), or MSPPOH (20 mg·kg^{-1}·day^{-1} iv) for 2 wk. At that point, the conscious MAP was significantly higher in the HF control group than in rats fed the control diet (139 ± 3 vs. 124 ± 2 mmHg, $P < 0.05$; Fig. 1). Fenofibrate significantly lowered the MAP of HF rats to 116 ± 4 mmHg; this effect was attenuated by fenofibrate + MSPPOH. Similarly, AUDA significantly lowered the blood pressure of HF rats to 119 ± 3 mmHg ($P < 0.05$). MSPPOH did not affect blood pressure in HF rats. Interestingly, fenofibrate, fenofibrate + MSPPOH, AUDA, and MSPPOH had no effect on blood pressure in age-matched rats fed the control diet (Fig. 1).

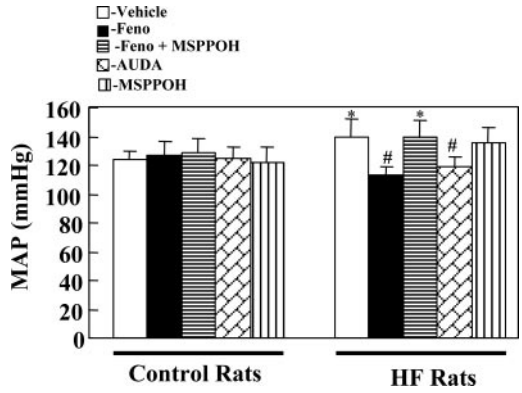

Fig. 1. Mean arterial pressure (MAP) in conscious 11-wk-old control rats and rats fed a high-fat diet (HF). Control and HF rats were treated for 2 wk with vehicle, fenofibrate (Feno, 30 mg·kg^{-1}·day^{-1} ig), fenofibrate (30 mg·kg^{-1}·day^{-1} ig) + *N*-methanesulfonyl-6-(2-proparyloxyphenyl)hexanamide (MSPPOH, 20 mg·kg^{-1}·day^{-1} iv), AUDA (50 mg/l in drinking water), or MSPPOH (20 mg·kg^{-1}·day^{-1} iv). Values are means ± SE ($n = 6$). *$P <$ 0.05 vs. control. #$P < 0.05$ vs. vehicle-treated HF rats.

Effects of fenofibrate, MSPPOH, and AUDA on renal hemodynamics in HF rats. In a preceding study, we showed that renal EET production was downregulated in HF rats (33). Here, to assess the effects of increased EETs on renal hemodynamics of HF rats, renal MAP, RBF, RVR, and GFR were examined in HF rats treated with vehicle, fenofibrate, fenofibrate + MSPPOH, or AUDA. As shown in Fig. 2, 2 wk of fenofibrate treatment elevated RBF (11.7 ± 2 vs. 9.6 ± 1 ml/min) but significantly reduced RVR (8.7 ± 1.2 vs. 13.3 ± 1.5 mmHg·ml^{-1}·min, $P < 0.05$) and GFR (1.2 ± 0.2 vs. 1.7 ± 0.2 ml/min, $P < 0.05$). The effects of fenofibrate on RBF and RVR were attenuated by addition of MSPPOH (Fig. 2). Similarly, 2 wk of AUDA treatment increased RBF but decreased RVR and GFR compared with vehicle-treated HF rats. Moreover, MSPPOH did not affect MAP, RBF, RVR, or GFR in HF rats (Fig. 2).

Effects of fenofibrate, MSPPOH, and AUDA on sodium balance in HF rats. To examine whether increased renal EET production affects sodium balance in HF rats, the cumulative sodium balance was determined for 15 days in 11-wk-old HF rats treated with vehicle, fenofibrate, fenofibrate + MSPPOH, or AUDA. As shown in Fig. 3, after 15 days of measurement, the cumulative sodium balance was significantly lower in the animals treated with fenofibrate (−0.87 ± 0.2 meq, $P < 0.05$) and AUDA (−0.48 ± 0.2 meq, $P < 0.05$) than in the vehicle control group (1.05 ± 0.1 meq). In the group treated with fenofibrate + MSPPOH, the cumulative sodium balance curve returned to the level in the vehicle-treated control group (Fig. 3). MSPPOH did not affect cumulative sodium balance in HF rats.

Effects of MSPPOH on renal cortical EET production in fenofibrate-treated HF rats. HPLC was used to examine renal cortical AA metabolism in HF rats treated with vehicle, fenofibrate, or fenofibrate + MSPPOH. Compared with the control group, fenofibrate significantly elevated renal epoxygenase activity (EET production): 232 ± 40 vs. 65 ± 30 pmol·mg^{-1}·min^{-1} ($P < 0.05$; Fig. 4). The fenofibrate-induced increase of renal epoxygenase activity was attenuated by fe-

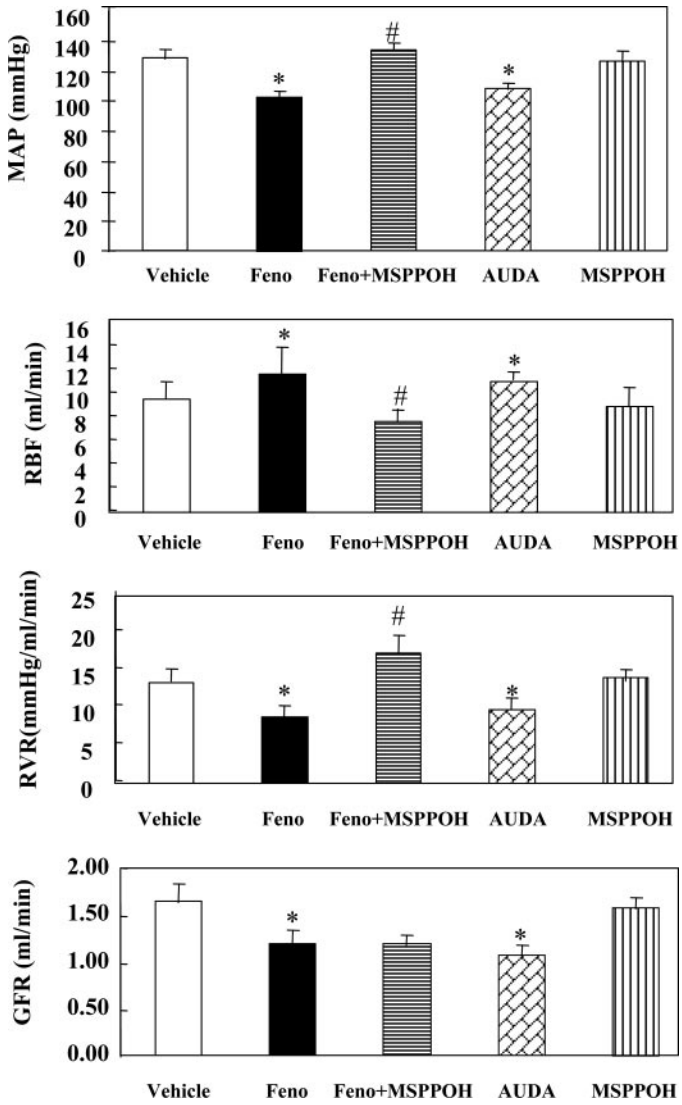

Fig. 2. MAP (*A*), renal blood flow (RBF, *B*), renal vascular resistance (RVR, *C*), and glomerular filtration rate (GFR, *D*) in 11-wk-old HF rats treated with vehicle, fenofibrate, fenofibrate + MSPPOH, AUDA, or MSPPOH. Values are means ± SE ($n = 6$). *$P < 0.05$ vs. vehicle-treated HF rats. #$P < 0.05$ vs. fenofibrate-treated HF rats.

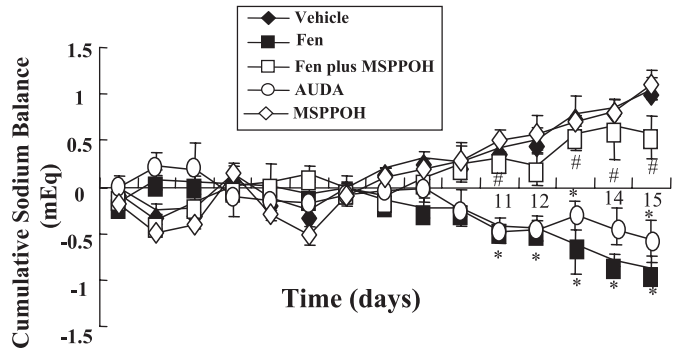

Fig. 3. Cumulative sodium balance in 11-wk-old HF rats treated with vehicle, fenofibrate (Fen), fenofibrate + MSPPOH, AUDA, or MSPPOH for 15 days. Values are means ± SE ($n = 6$). *$P < 0.05$ vs. vehicle-treated HF rats. #$P < 0.05$ vs. fenofibrate-treated HF rats.

nofibrate + MSPPOH (Fig. 4). However, fenofibrate or fenofibrate + MSPPOH had no effect on cortical ω-hydroxylase activity (20-HETE production).

Effects of MSPPOH on expression of renal CYP epoxygenases in fenofibrate-treated HF rats. Western blot analysis was used to examine the expression of CYP2C23, CYP2C11, and CYP2J in HF rats treated with vehicle, fenofibrate, or fenofibrate + MSPPOH. Fenofibrate significantly induced CYP2C23, CYP2C11, and CYP2J expression in the renal cortex and renal microvessels (Fig. 5). Densitometry analysis normalized with β-actin showed a 45% increase in CYP2C23 [4.8 ± 0.1 vs. 3.3 ± 0.03 arbitrary units (AU), $n = 3$, $P < 0.05$], a 46% increase in CYP2C11 (3.8 ± 0.6 vs. 2.6 ± 0.6 AU, $n = 3$, $P < 0.05$), and a 40% increase in CYP2J (4.2 ± 0.2 vs. 3.0 ± 0.03 AU, $n = 3$, $P < 0.05$) expression in the renal cortex of fenofibrate-treated HF rats compared with the vehicle-treated HF group. Similarly, fenofibrate increased the expression of CYP2C23 by 63% (1.3 ± 0.06 vs. 0.8 ± 0.2 AU, $n = 3$, $P < 0.05$), CYP2C11 by 83% (1.1 ± 0.02 vs. 0.6 ± 0.01 AU, $n = 3$, $P < 0.05$), and CYP2J by 45% (2.9 ± 0.1 vs. 2.0 ± 0.02 AU, $n = 3$, $P < 0.05$) in renal microvessels. The induction effects of fenofibrate on CYP epoxygenases in the renal cortex and microvessels were somewhat attenuated by fenofibrate + MSPPOH (Fig. 5).

To substantiate these results, immunohistochemical analysis of CYP2C23, CYP2C11, and CYP2J was also performed in renal sections from HF rats treated with vehicle, fenofibrate, or fenofibrate + MSPPOH. The most intense staining was observed in renal tubules, whereas glomeruli showed a low immunoreaction to these CYP isoforms. The staining intensity showed a 135% increase in CYP2C23 (24.7 ± 2 vs. 10.5 ± 2 AU, $n = 4$, $P < 0.05$), a 117% increase in CYP2C11 (25.8 ± 3 vs. 11.9 ± 1 AU, $n = 4$, $P < 0.05$), and a 115% increase in CYP2J (11.4 ± 1 vs. 5.3 ± 2 AU, $n = 4$, $P < 0.05$) expression in the fenofibrate-treated group. The induction effects of fenofibrate on CYP epoxygenases were attenuated by fenofibrate + MSPPOH (Fig. 6). No immunohistochemical staining was observed in a negative control section (Fig. 6).

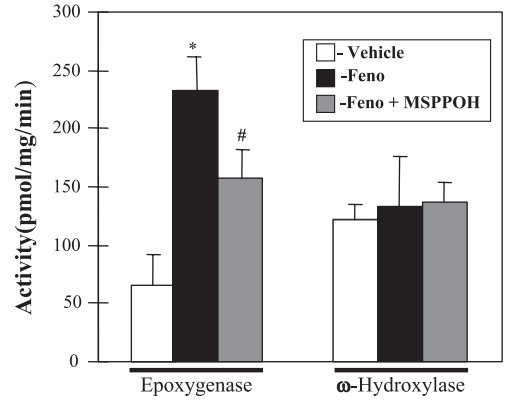

Fig. 4. Effect of fenofibrate and MSPPOH on renal cortical epoxygenase and ω-hydroxylase activities in HF rats treated with vehicle, fenofibrate, or fenofibrate + MSPPOH. Epoxygenase activity was determined from the sum of DHET and EET formation; ω-hydroxylase activity was determined from 20-HETE formation. Values are means ± SE ($n = 4$). *$P < 0.05$ vs. vehicle-treated HF rats. #$P < 0.05$ vs. fenofibrate-treated HF rats.

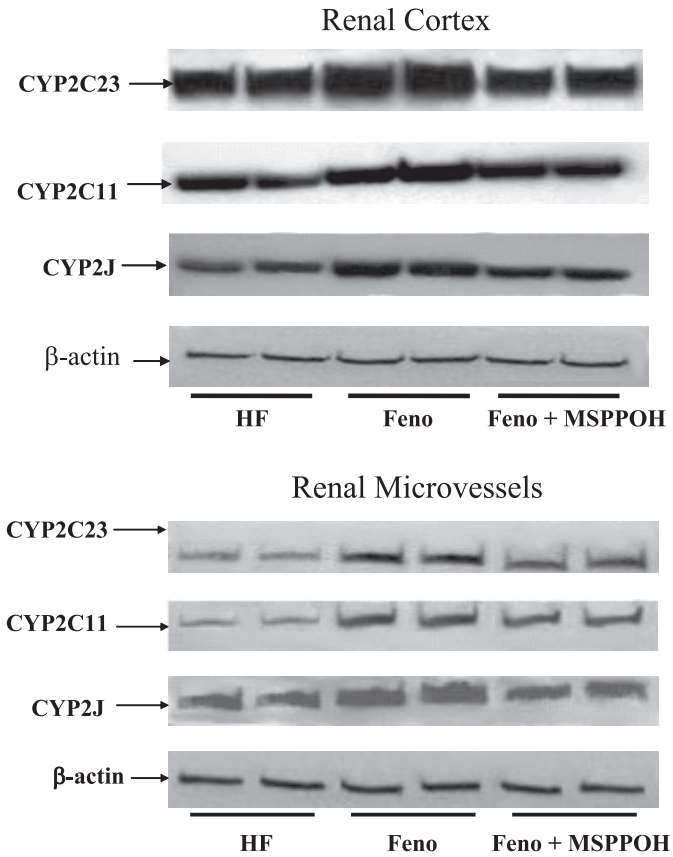

Fig. 5. Representative Western blots of CYP2C23, CYP2C11, CYP2J, and β-actin in renal cortical microsomes and renal microvessel homogenates isolated from HF rats treated with vehicle, fenofibrate, or fenofibrate + MSPPOH.

DISCUSSION

In a previous study, we demonstrated significant downregulation of EET production and CYP2C23 expression in the renal tissues of rats fed an HF diet for 10 wk (42). The downregulation of renal tubular EET production is associated with hypertension, abnormal renal hemodynamics, and sodium retention (41). To substantiate these findings, we postulated that the increased production of EETs by fenofibrate and AUDA can affect blood pressure, renal hemodynamics, and sodium retention in HF rats. This study demonstrates that fenofibrate selectively increases AA epoxidation activity but does not affect ω-hydroxylase activity in renal cortical microsomes isolated from HF rats (Fig. 4). Western blot (Fig. 5) and immunohistochemical (Fig. 6) results showed that CYP2C11, CYP2C23, and CYP2J expression was also significantly elevated in the renal cortex and renal microvessels after fenofibrate treatment. Interestingly, fenofibrate-induced increases in renal CYP epoxgenase activity and expression are associated with renal functional changes, including decreased MAP, RVR, GFR, and cumulative sodium balance but increased RBF. Although fenofibrate + MSPPOH attenuates the effects of fenofibrate on renal functional parameters in HF rats, fenofibrate + MSPPOH cannot return epoxygenase activity to the levels of the vehicle control group (Fig. 4). The reason for this is not clear, but it could be that the dose we used for MSPPOH is not the maximal dose for HF rats. A higher dose of MSPPOH may be required to completely block the induction effects of fenofibrate on epoxygenase activity in HF rats.

Fenofibrate is a peroxisome proliferator-activated receptor-α (PPAR-α) agonist; it upregulates many genes involved in fatty acid oxidation, such as acyl-CoA oxidase, carnitine palmitoyl transferase I, and CYP4A isoforms, through the activation of PPAR-α (29). Because of these biological activities, PPAR-α agonists such as fenofibrate have been used to lower triglycerides in dyslipidemic patients. In addition to its antihyperlipidemic effect, fenofibrate has been shown to reduce blood pressure in different hypertensive animal models (31, 35). For example, Wilson et al. (35) showed that fenofibrate significantly reduced MAP in Dahl salt-sensitive rats treated with a high-salt diet, and Vera et al. (31) showed that fenofibrate decreased MAP from 144 to 115 mmHg in angiotensin II-treated mice. Both of these reports showed that fenofibrate induced renal 20-HETE production, suggesting that the antihypertensive effects of fenofibrate are due to the induction of renal 20-HETE. In the present study, we observed a significant increase of renal CYP epoxygenase activity, rather than an increase of ω-hydroxylase activity, by fenofibrate in HF rats (Fig. 4). This is consistent with the results of Muller et al. (20), who showed selectively increased renal CYP epoxygenase activity as a result of fenofibrate treatment of male rats. The reason for the inconsistency between some previous results (31, 35) and our results is not known but could be a consequence of procedural differences. For example, we administered 30 $mg \cdot kg^{-1} \cdot day^{-1}$ of fenofibrate for 2 wk, whereas others used 95 $mg \cdot kg^{-1} \cdot day^{-1}$ for 3 wk (35).

Although we observed the induction of CYP epoxygenase expression levels in renal tissues in response to fenofibrate treatment (Figs. 5 and 6), it is not clear whether fenofibrate can increase endogenous EET levels in the kidneys. The main reason for this statement is that PPAR-α agonists, such as clofibrate and fenofibrate, are also good inducers of sEH (10). Hammock and Ota (10) first demonstrated that chronic clofibrate treatment in mice significantly increased hepatic sEH activity. Similarly, Schladt et al. (26) demonstrated that fenofibrate increased hepatic and renal sEH activity eight- and twofold, respectively, in rats. Since sEH is the enzyme responsible for the conversion of EETs to DHETs (21), it is possible that chronic treatment with fenofibrate also induces sEH levels and activity in the kidneys of HF rats, resulting in increased degradation of EETs, which eliminates induction effects of CYP epoxygenases by fenofibrate. Further investigation of the effects of fenofibrate on renal vascular and tubular sEH levels and activity in HF rats is required.

Since DHETs are much more polar than EETs and are considered to have reduced biological activity, whereas the inhibition of sEH stabilizes EET levels, inhibition of sEH can be a good approach to study the physiological function of EETs. Many sEH inhibitors have been developed to facilitate long-term in vivo studies. These inhibitors are competitive and have efficiently decreased the degradation of EETs in several in vivo models (21). AUDA, an sEH inhibitor containing an *N′*-carboxylic acid moiety, increases water solubility without significantly reducing the potency of sEH inhibition (21). Recently, AUDA was used to study the anti-inflammatory effects of EETs in endothelial cells (19), the effects of EETs in the brain on the regulation of blood pressure in spontaneously hypertensive rats (28), and the antihypertensive effects of

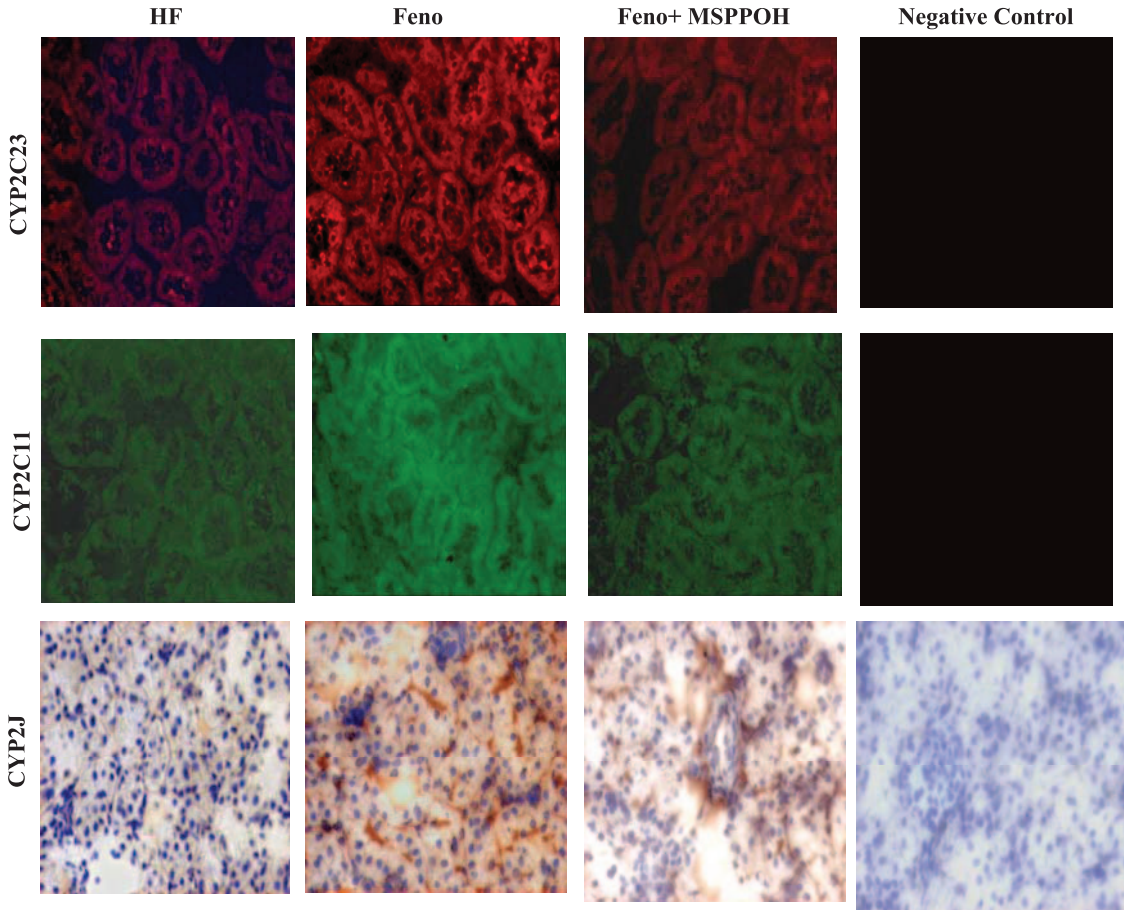

Fig. 6. Immunohistochemical analysis of CYP2C23, CYP2C11, and CYP2J in renal sections from HF rats treated with vehicle, fenofibrate, or fenofibrate + MSPPOH. CYP2C23 was detected by tetramethylrhodamine (red), CYP2C11 by FITC (green), and CYP2J by diaminobenzidine (brown). The same procedure was used for negative control slides, but they were not incubated with primary antibody.

EETs in a salt-sensitive hypertensive model (16). Using a protocol similar to that described in the literature (16), we found that AUDA decreased MAP and RVR but increased RBF in HF rats (Fig. 2). The effects of EETs on the renal hemodynamics of AUDA-treated HF rats could be due to the endothelial actions of EETs. EETs have been identified as endothelium-derived hyperpolarizing factors (14, 24) that are distinct from nitric oxide and prostacyclin. They are produced within and released from endothelial cells in response to physical and pharmacological stimuli. EETs then diffuse to vascular smooth muscle cells to hyperpolarize the cell membrane and cause relaxation (7). Thus, increasing the levels of EETs by the administration of AUDA can cause dilation and decreased resistance of renal blood vessels (Fig. 2) and, thereby, contribute to the correction of abnormal renal hemodynamics in obese HF rats.

Although the precise mechanisms whereby obesity causes hypertension are not clear, a review by Hall (8) has suggested that the kidney is the central player and that sodium retention is a major mechanism in obesity-induced hypertension. Interestingly, we have found that the development of hypertension in HF rats is associated with increased cumulative sodium balance (Fig. 3), which is a good index of sodium retention. The stabilization of EET production by AUDA attenuates sodium retention in HF rats (Fig. 3). These results are consistent with the finding by Jung et al. (18) that AUDA treatment was accompanied by increased urinary sodium excretion in angiotensin II-treated mice. Although the mechanism whereby the increased EET level attenuates sodium retention is not clear, it is possible that this occurs as a consequence of the action of EETs on sodium transport in the nephron. For example, EETs have been shown to inhibit Na^+-K^+-ATPase activity and are involved in the regulation of sodium transport in proximal tubules (24). In addition, Wei et al. (34) demonstrated that, in the cortical collecting duct, EET directly inhibits the activity of epithelial sodium channels (ENaC). It is possible, therefore, that AUDA increases EET levels in renal tubular segments and inhibits the activity of these sodium transporters, thus causing natriuresis and attenuating sodium retention. Alternatively, changes in the trafficking of sodium transport proteins in the nephron could be responsible. Dos Santos et al. (6) demonstrated that increased production of CYP eicosanoids by the elevation of renal perfusion pressure increases urinary sodium excretion and promotes the internalization of sodium/hydrogen exchanger type 3 in proximal tubular cells. It is possible that AUDA-induced reduced EET degradation affects the trafficking of sodium transporters in different segments of nephron, which then contributes to the reduction of sodium retention. All these mechanisms deserve further investigation.

In the present study, we focused on the effect of increased levels of EETs caused by AUDA treatment in kidneys on renal function and blood pressure in HF rats. Since we administered AUDA systemically, it is possible that AUDA can also upregulate levels of EETs in other organs and contribute to cardiovascular hemodynamic changes such as total peripheral resistance and cardiac output. This possibility is supported by significant biological activity of EETs in the heart and brain (24). Interestingly, Jung et al. (18) recently demonstrated that intravenous injection of AUDA significantly lowered blood pressure and heart rate in angiotensin II-induced mice. However, the reasons for the effects of increased EET production on cardiac function are not clear. It will be interesting to study whether the increased levels of EETs caused by AUDA can affect cardiac function and cardiovascular hemodynamics in HF rats.

The results of any pharmacological agent must be interpreted with caution. MSPPOH appears to be very selective as an epoxygenase inhibitor, as does as AUDA as an inhibitor of sEH. However, there could be undescribed activities. Furthermore, the downstream effects of the inhibition of these enzymes can be complex. PPAR-α agonists have more far-reaching effects. Other studies have shown that PPAR-α agonists increase renal ω-hydroxylase activity, resulting in increased 20-HETE production (24). In many cases, this increases inflammation and hypertension. All PPAR-α agonists that have been studied in rodents are strong inducers of sEH (10), resulting in a decrease in EET levels and, thus, an increase in inflammation and hypertension. Our observation that fenofibrate reduces MAP and has the associated beneficial effects on renal hemodynamics suggests that the increase in biosynthesis of EETs and possible other regulatory lipids resulting from fenofibrate treatment overshadows the effects of possible increases of 20-HETE production and sEH-induced EET degradation. Our data also suggest that, in rodents, combined dosing of sEH inhibitor with compounds such as fenofibrate, which increase the biosynthesis of epoxylipids, should have a positive effect.

In summary, we have demonstrated that HF-induced hypertension is associated with abnormal renal hemodynamics and increased cumulative sodium balance. We also have shown that fenofibrate selectively increases CYP epoxygenase activity and that the effects of fenofibrate are associated with the induction of CYP2C and CYP2J in renal tubules and microvessels. The inducing effects of fenofibrate on the expression of CYP epoxygenases were attenuated by fenofibrate + MSPPOH, a selective EET biosynthesis inhibitor. Treatment with fenofibrate and AUDA decreased sodium balance, RVR, GFR, and blood pressure in HF rats. Moreover, the effects of fenofibrate on renal hemodynamics and sodium balance were attenuated by MSPPOH. This study demonstrates that stabilization of the renal EET pathway affects renal function and blood pressure in HF rats and that EET biosynthesis may have important functional implications in obesity.

ACKNOWLEDGMENTS

The authors thank Jeanne Cole for editorial assistance.

GRANTS

This study was supported by National Heart, Lung, and Blood Institute Grants R01 HL-70887 and HL-082733 (to M.-H. Wang) and National Institute of Diabetes and Digestive and Kidney Diseases Grant DK-38226 and a grant from the Robert A. Welch Foundation (to J. R. Falck). Partial support was provided by National Institutes of Health Grants ES-02710, ES-05707, and HL-078016 (to B. D. Hammock).

REFERENCES

1. **Baylis C, Samsell L, Racusen L, Gladfelter W.** Hypothalamic lesions induce obesity and sex-dependent glomerular damage and increases in blood pressure in rats. *Hypertension* 27: 926–932, 1996.
2. **Da Silva AA, Kuo JJ, Tallam LS, Hall JE.** Role of endothelin-1 in blood pressure regulation in a rat model of visceral obesity and hypertension. *Hypertension* 43: 383–387, 2004.
3. **Dobrian AD, Davies MJ, Prewitt RL, Lauterio TJ.** Development of hypertension in a rat model of diet-induced obesity. *Hypertension* 35: 1009–1015, 2000.
4. **Dobrian AD, Schriver AD, Lynch T, Prewitt RL.** Effects of salt on hypertension and oxidative stress in a rat model of diet-induced obesity. *Am J Physiol Renal Physiol* 285: F619–F628, 2003.
5. **Dorrance AM, Rupp N, Pollock DM, Newman JW, Hammock BD, Imig JD.** An epoxide hydrolase inhibitor, 12-(3-adamantan-1-yl-ureido) dodecanoic acid (AUDA), reduces ischemic cerebral infarct size in stroke-prone spontaneously hypertensive rats. *J Cardiovasc Pharmacol* 46: 842–848, 2005.
6. **Dos Santos EA, Dahly-Vernon AJ, Hoagland KM, Roman RJ.** Inhibition of the formation of EETs and 20-HETE with 1-aminobenzotriazole attenuates pressure natriuresis. *Am J Physiol Regul Integr Comp Physiol* 287: R58–R68, 2004.
7. **Fleming I.** Cytochrome P450 epoxygenases as EDHF synthase(s). *Pharmacol Res* 49: 525–533, 2004.
8. **Hall JE.** The kidney, hypertension, obesity. *Hypertension* 41: 625–633, 2003.
9. **Hall JE, Brands MW, Dixon WN, Smith MJ Jr.** Obesity-induced hypertension. Renal function and systemic hemodynamics. *Hypertension* 22: 292–299, 1993.
10. **Hammock BD, Ota K.** Differential induction of cytosolic epoxide hydrolase, microsomal epoxide hydrolase, and glutathione *S*-transferase activities. *Toxicol Appl Pharmacol* 71: 254–265, 1983.
11. **Holla VR, Makita K, Zaphiropoulos PG, Capdevila JH.** The kidney cytochrome *P*-450 2C23 arachidonic acid epoxygenase is upregulated during dietary salt loading. *J Clin Invest* 104: 751–760, 1999.
12. **Huang H, Chang HH, Xu Y, Reddy DS, Du J, Zhou Y, Dong Z, Falck JR, Wang MH.** Epoxyeicosatrienoic acid inhibition alters renal hemodynamics during pregnancy. *Exp Biol Med (Maywood)* 231: 1744–1752, 2006.
13. **Imig JD.** Eicosanoid regulation of the renal vasculature. *Am J Physiol Renal Physiol* 279: F965–F981, 2000.
14. **Imig JD.** Epoxide hydrolase and epoxygenase metabolites as therapeutic targets for renal diseases. *Am J Physiol Renal Physiol* 289: F496–F503, 2005.
15. **Imig JD, Zhao X, Capdevila JH, Morisseau C, Hammock BD.** Soluble epoxide hydrolase inhibition lowers arterial blood pressure in angiotensin II hypertension. *Hypertension* 39: 690–694, 2002.
16. **Imig JD, Zhao X, Zaharis CZ, Olearczyk JJ, Pollock DM, Newman JW, Kim IH, Watanabe T, Hammock BD.** An orally active epoxide hydrolase inhibitor lowers blood pressure and provides renal protection in salt-sensitive hypertension. *Hypertension* 46: 975–981, 2005.
17. **Jin L, Foss CE, Zhao X, Mills TM, Wang MH, McCluskey LP, Yaddanapud GS, Falck JR, Imig JD, Webb RC.** Cytochrome P450 epoxygenases provide a novel mechanism for penile erection. *FASEB J* 20: 539–541, 2006.
18. **Jung O, Brandes RP, Kim IH, Schweda F, Schmidt R, Hammock BD, Busse R, Fleming I.** Soluble epoxide hydrolase is a main effector of angiotensin II-induced hypertension. *Hypertension* 45: 759–765, 2005.
19. **Liu Y, Zhang Y, Schmelzer K, Lee TS, Fang X, Zhu Y, Spector AA, Gill S, Morisseau C, Hammock BD, Shyy JY.** The anti-inflammatory effect of laminar flow: the role of PPARγ, epoxyeicosatrienoic acids, and soluble epoxide hydrolase. *Proc Natl Acad Sci USA* 102: 16747–16752, 2005.
20. **Muller DN, Theuer J, Shagdarsuren E, Kaergel E, Honeck H, Park JK, Markovic M, Barbosa-Sicard E, Dechend R, Wellner M, Kirsch T, Fiebeler A, Rothe M, Haller H, Luft FC, Schunck WH.** A peroxisome proliferator-activated receptor-α activator induces renal CYP2C23 activity and protects from angiotensin II-induced renal injury. *Am J Pathol* 164: 521–532, 2004.

21. **Newman JW, Morisseau C, Hammock BD.** Epoxide hydrolases: their roles and interactions with lipid metabolism. *Prog Lipid Res* 44: 1–51, 2005.
22. **Ogungbade GO, Akinsanmi LA, Jiang H, Oyekan AO.** Role of epoxyeicosatrienoic acids in renal functional response to inhibition of NO production in the rat. *Am J Physiol Renal Physiol* 285: F955–F964, 2003.
23. **Qi Z, Whitt I, Mehta A, Jin J, Zhao M, Harris RC, Fogo AB, Breyer MD.** Serial determination of glomerular filtration rate in conscious mice using FITC-inulin clearance. *Am J Physiol Renal Physiol* 286: F590–F596, 2004.
24. **Roman RJ.** *P*-450 metabolites of arachidonic acid in the control of cardiovascular function. *Physiol Rev* 82: 131–185, 2002.
25. **Scarborough PE, Ma J, Qu W, Zeldin DC.** P450 subfamily CYP2J and their role in the bioactivation of arachidonic acid in extrahepatic tissues. *Drug Metab Rev* 31: 205–234, 1999.
26. **Schladt L, Hartmann R, Timms C, Strolin-Benedetti M, Dostert P, Worner W, Oesch F.** Concomitant induction of cytosolic but not microsomal epoxide hydrolase with peroxisomal β-oxidation by various hypolipidemic compounds. *Biochem Pharmacol* 36: 345–351, 1987.
27. **Schmelzer KR, Kubala L, Newman JW, Kim IH, Eiserich JP, Hammock BD.** Soluble epoxide hydrolase is a therapeutic target for acute inflammation. *Proc Natl Acad Sci USA* 102: 9772–9777, 2005.
28. **Sellers KW, Sun C, ez-Freire C, Waki H, Morisseau C, Falck JR, Hammock BD, Paton JF, Raizada MK.** Novel mechanism of brain soluble epoxide hydrolase-mediated blood pressure regulation in the spontaneously hypertensive rat. *FASEB J* 19: 626–628, 2005.
29. **Simpson AE.** The cytochrome P450 4 (CYP4) family. *Gen Pharmacol* 28: 351–359, 1997.
30. **Spector AA, Fang X, Snyder GD, Weintraub NL.** Epoxyeicosatrienoic acids (EETs): metabolism and biochemical function. *Prog Lipid Res* 43: 55–90, 2004.
31. **Vera T, Taylor M, Bohman Q, Flasch A, Roman RJ, Stec DE.** Fenofibrate prevents the development of angiotensin II-dependent hypertension in mice. *Hypertension* 45: 730–735, 2005.
32. **Wang MH, Brand-Schieber E, Zand BA, Nguyen X, Falck JR, Balu N, Laniado Schwartzman M.** Cytochrome P450-derived arachidonic acid metabolism in the rat kidney: characterization of selective inhibitors. *J Pharmacol Exp Ther* 284: 966–973, 1998.
33. **Wang MH, Smith A, Zhou Y, Chang HH, Lin S, Zhao X, Imig JD, Dorrance AM.** Downregulation of renal CYP-derived eicosanoid synthesis in rats with diet-induced hypertension. *Hypertension* 42: 594–599, 2003.
34. **Wei Y, Lin DH, Kemp R, Yaddanapudi GS, Nasjletti A, Falck JR, Wang WH.** Arachidonic acid inhibits epithelial Na channel via cytochrome P450 (CYP) epoxygenase-dependent metabolic pathways. *J Gen Physiol* 124: 719–727, 2004.
35. **Wilson TW, Alonso-Galicia M, Roman RJ.** Effects of lipid-lowering agents in the Dahl salt-sensitive rat. *Hypertension* 31: 225–231, 1998.
36. **Wu S, Chen W, Murphy E, Gabel S, Tomer KB, Foley J, Steenbergen C, Falck JR, Moomaw CR, Zeldin DC.** Molecular cloning, expression, and functional significance of a cytochrome P450 highly expressed in rat heart myocytes. *J Biol Chem* 272: 12551–12559, 1997.
37. **Xu D, Li N, He Y, Timofeyev V, Lu L, Tsai HJ, Kim IH, Tuteja D, Mateo RK, Singapuri A, Davis BB, Low R, Hammock BD, Chiamvimonvat N.** Prevention and reversal of cardiac hypertrophy by soluble epoxide hydrolase inhibitors. *Proc Natl Acad Sci USA* 103: 18733–18738, 2006.
38. **Zhang QY, Ding X, Kaminsky LS.** cDNA cloning, heterologous expression, and characterization of rat intestinal CYP2J4. *Arch Biochem Biophys* 340: 270–278, 1997.
39. **Zhao X, Yamamoto T, Newman JW, Kim IH, Watanabe T, Hammock BD, Stewart J, Pollock JS, Pollock DM, Imig JD.** Soluble epoxide hydrolase inhibition protects the kidney from hypertension-induced damage. *J Am Soc Nephrol* 15: 1244–1253, 2004.
40. **Zhou Y, Chang HH, Du J, Wang CY, Dong Z, Wang MH.** Renal epoxyeicosatrienoic acid synthesis during pregnancy. *Am J Physiol Renal Physiol* 288: F221–F226, 2005.
41. **Zhou Y, Huang H, Chang HH, Du J, Wu JF, Wang CY, Wang MH.** Induction of renal 20-hydroxyeicosatetraenoic acid by clofibrate attenuates high-fat diet-induced hypertension in rats. *J Pharmacol Exp Ther* 317: 11–18, 2006.
42. **Zhou Y, Lin S, Chang HH, Du J, Dong Z, Dorrance AM, Brands MW, Wang MH.** Gender differences of renal CYP-derived eicosanoid synthesis in rats fed a high-fat diet. *Am J Hypertens* 18: 530–537, 2005.